

LETTER • OPEN ACCESS

## Robust changes to the wettest and driest days of the year are hidden within annual rainfall projections: a New Zealand case study

To cite this article: Luke J Harrington *et al* 2024 *Environ. Res. Lett.* **19** 074057

View the [article online](#) for updates and enhancements.

You may also like

- [A framework to incorporate spatiotemporal variability of rainfall extremes in summer monsoon declaration in India](#)  
Vimal Mishra, Amar Deep Tiwari and Rohini Kumar
- [Urbanization alters rainfall extremes over the contiguous United States](#)  
Jitendra Singh, Subhankar Karmakar, Debasish PaiMazumder *et al.*
- [The contribution of precipitation recycling to North American wet and dry precipitation extremes](#)  
Christopher B Skinner, Tyler S Harrington, Mathew Barlow *et al.*

# Breath Biopsy Conference

BREATH BIOPSY

Join the conference to explore the **latest challenges** and advances in **breath research**, you could even **present your latest work!**



5th & 6th November  
Online



Main talks



Early career sessions



Posters

Register now for free!

ENVIRONMENTAL RESEARCH  
LETTERS

## LETTER

## OPEN ACCESS




RECEIVED  
16 April 2024REVISED  
10 June 2024ACCEPTED FOR PUBLICATION  
14 June 2024PUBLISHED  
2 July 2024

Original content from  
this work may be used  
under the terms of the  
[Creative Commons  
Attribution 4.0 licence](#).

Any further distribution  
of this work must  
maintain attribution to  
the author(s) and the title  
of the work, journal  
citation and DOI.



## Robust changes to the wettest and driest days of the year are hidden within annual rainfall projections: a New Zealand case study

Luke J Harrington<sup>1,\*</sup> , Suzanne M Rosier<sup>2</sup>, Tom I Marsh<sup>3</sup>  and Dave J Frame<sup>3</sup> <sup>1</sup> Te Aka Mātuatua School of Science, University of Waikato, Hillcrest Road, Hamilton 3216, New Zealand<sup>2</sup> National Institute of Water and Atmospheric Research, PO Box 8602, Christchurch 8440, New Zealand<sup>3</sup> School of Physical and Chemical Sciences, University of Canterbury, Christchurch, New Zealand

\* Author to whom any correspondence should be addressed.

E-mail: [luke.harrington@waikato.ac.nz](mailto:luke.harrington@waikato.ac.nz)**Keywords:** rainfall unevenness, rainfall extremes, large-ensemble modelling, climate change, New ZealandSupplementary material for this article is available [online](#)

## Abstract

Understanding how the statistical properties of daily rainfall will respond to a warming climate requires ensembles of climate model data which are much larger than those typically available from existing centennial-scale modelling experiments. While such centennial-scale experiments are very useful to explore scenario uncertainty in twenty-first century climate, ensemble size constraints often result in regional climate change assessments restricting their focus to annual- or season-mean rainfall projections without providing robust information about changes to the most extreme events. Here, we make use of multi-thousand member ensembles of regional climate model output from the *Weather@Home* project to explicitly resolve how the wettest and driest days of the year over New Zealand will respond to simulations of a 3 °C world, relative to simulations of the climate of the recent past (2006–15). Using a novel framework to disentangle changes during the wettest and driest days of the year, we show that many regions which show negligible change in annual mean rainfall are in fact experiencing significant changes in the amount of rain falling during both the wettest and driest spells. Exploring these changes through the lens of drought risk, we find many agricultural regions in New Zealand will face significant changes in the frequency of low-rainfall extremes in a warmer world.

## 1. Introduction

Understanding the unevenness of precipitation is critically important when anticipating and adapting to the risks associated with a hydrological cycle which is strengthening due to anthropogenic climate change (Giorgi *et al* 2011, Padrón *et al* 2020, Gudmundsson *et al* 2021). Seminal work by Pendergrass and colleagues (Pendergrass *et al* 2017, Pendergrass 2018, Pendergrass and Knutti 2018) has brought attention to the sometimes extreme asymmetry which can be observed in daily precipitation, as well as its consequences. For example, previous research has found that globally, in the median case, half of annual precipitation falls within the wettest twelve days (Pendergrass and Knutti 2018), with most future increases in annual precipitation also concentrated

within these wettest days of the year. Complementary work by Goffin and colleagues (2024) examined temporal changes in how many of the wettest days are required to contribute to half of a year's annual rainfall, revealing that precipitation regimes have intensified over continental Europe within the last fifty years. Equally, the importance of the many other days of the year with little precipitation (or 'drizzle days') cannot be overlooked, as their presence or absence can be a critical determinant of potential drought risk and subsequent impacts (Fishman 2016, Sloat *et al* 2018, Lesk *et al* 2022).

While past research on the unevenness of daily precipitation and its change through time has primarily focused on the analysis of historical observations or multi-model projections of future climate, few studies have leveraged the recent growth

of large-ensemble climate modelling experiments (Deser *et al* 2020, Lehner *et al* 2020). Relatedly, one of the drawbacks of previous studies on daily rainfall asymmetry has been the tendency to focus only on the wettest days of the year required to reach some fraction of annual rainfall, rather than considering changes to unevenness at both the dry and wet end of a location's precipitation regime: this, in turn, relates to the sample size limitations inherent in analyses relying on single observational datasets or from climate model experiments with small ensemble sizes, like the fifth (or sixth) phase of the Coupled Model Intercomparison Project (CMIP5; Taylor *et al* 2012, Eyring *et al* 2016).

In this study, we will leverage very large (multi-thousand member) ensembles of regional climate model output from one of the largest initial-condition climate modelling experiments—*Weather@Home*—to interrogate changes to the unevenness of daily rainfall over the New Zealand region. Understanding any changes to the asymmetry in daily rainfall through time is particularly pertinent for a temperate, mid-latitude and topographically complex country like New Zealand, a country with a large primary sector which relies primarily on rain-fed pastoral agriculture, and which has a diverse array of rainfall regimes which can differ significantly over short distances (Sturman and Tapper 2006).

Previous modelling efforts to quantify changes in daily rainfall characteristics in response to a warming climate over New Zealand have been limited by model fidelity issues and computational cost constraints impeding the size of the ensembles used (Ministry for the Environment 2018). Consequently, there has been a focus on simple metrics of future precipitation change which are less sensitive to such model- and initial-condition uncertainties, particularly a focus on changes in total rainfall over individual seasons and annually (for example, <https://ofcnz.niwa.co.nz/>). Unfortunately, such coarsening of the temporal resolution of future climate projections often diminishes the practical utility for on-the-ground users of this information (Cradock-Henry *et al* 2018, Harrington 2021).

By explicitly quantifying how the intensity of rainfall is changing for each calendar day of the year, this study will examine how both the wettest and driest days of the year are projected to respond differently to additional anthropogenic climate change across New Zealand, as well as how these changes manifest themselves in the form of unprecedented dry years in the future.

## 2. Data and methods

### 2.1. Weather@Home simulations

The study makes use of the many thousands of simulations available from the *Weather@Home* regional climate modelling experiment for the

Australia-New Zealand region (Black *et al* 2016). The *Weather@Home* experiment (Massey *et al* 2015) enables such large ensembles to be created by employing volunteer distributed computing via the 'climateprediction.net' project (Allen 1999) using the 'BOINC' (Berkeley Open Infrastructure for Network Computing) platform (Anderson 2020). A volunteer participant downloads and runs two U.K. Met. Office Hadley Centre models in tandem: the global model HadAM3P (Pope *et al* 2000) with the regional model HadRM3P (Jones *et al* 2004) one-way nested within it. Both models are of the atmosphere only and are supplied with sea surface temperatures and sea ice as lower boundary conditions: here, these were taken from the OSTIA (Operational Sea surface Temperature and sea Ice Analysis) dataset (Donlon *et al* 2012).

To simulate near-present-day conditions (approximately equivalent to 0.9 K of warming above pre-industrial levels), the model set-up was run with all inputs—e.g. greenhouse gases, aerosol, ozone, solar and volcanic forcings—appropriate to near-present-day conditions. Simulations were performed in one-year lengths and covered the period 2006–15. Note that the model uses a 360 day year which has been carried forward into all calculations presented here.

Simulations of a world 3 K warmer than pre-industrial levels were performed by utilising the 'HAPPI' (Half a degree Additional warming: Prognosis and Projected Impacts) framework (Mitchell *et al* 2017) which was then expanded by Lo *et al* (2019) and Shiogama *et al* (2020). We input anthropogenic forcings (including well-mixed greenhouse gas concentrations) based on a weighted combination of the Representative Concentration Pathways (RCPs) 4.5 and 8.5 in 2095 ( $0.686 \times \text{RCP4.5} + 0.314 \times \text{RCP8.5}$ ), which leads to a global mean temperature response about 2.1 °C warmer than the 2006–15 ensemble mean (and thus 3 K above pre-industrial levels). Similarly, SST changes were taken from a multi-model mean of CMIP5 model simulations of 2091–2100 using a linear weighted combination of RCPs 4.5 and 8.5. Sea ice changes were estimated by applying a linear SST/sea ice relationship derived from observations to the SST changes (Mitchell *et al* 2017).

In this way, two sets of model simulations are produced: a baseline climatology (the 'Current Climate' experiment) covering the period 2006–15, and a 3 K warmer future (the '3 K experiment'), covering the 2090s (though in principle, it could represent any decade so long as the radiative forcings were consistent with a 3 °C-warmer world). In each case the decade is made up of one-year simulations, with the model being re-initialised for each year. Within each specification of supplied boundary conditions (i.e. a specific year within the present-day or 3 K future), the very large ensembles are created by introducing a small perturbation to the initial conditions

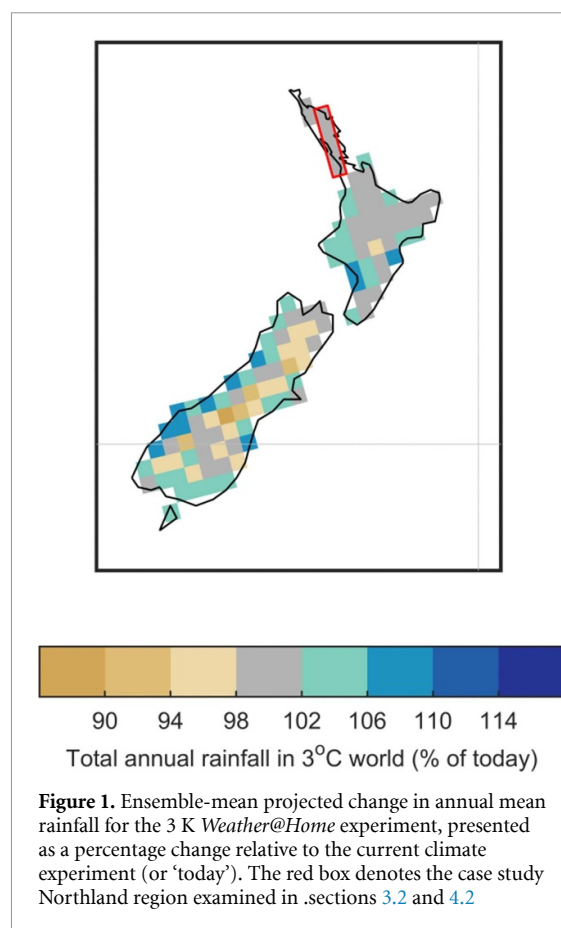
of the global climate model in the form of slight changes to the three-dimensional potential temperature field alongside perturbations to the large-scale circulation and soil moisture fields (these perturbations were generated by calculating the next-day differences within a one-year integration of the global model). Although these initial condition perturbations are only applied to the global model, they immediately affect the regional simulations through the transfer of lateral boundary conditions at the end of the first global model day (see Black *et al* 2016 for further details). Hence, these large ensembles represent many different realisations of possible weather states pertaining to any particular set of forcings, and in this way mimic the chaotic element inherent in the development of weather and climate features. More than 200 realisations of each year were run, leading to total ensemble sizes of 3662 and 2535 model years, respectively, for the Current Climate and 3 K experiments (see also table S1).

The *Weather@Home* model used here ran the global model at approximately 150 km resolution, with the embedded regional model spanning the Australasian domain developed by the Coordinated Regional Downscaling Experiment Australasia project (Evans *et al* 2021) at approximately 50 km resolution. The model evaluation performed by Black and colleagues (2016) demonstrated that this model set-up is capable of reproducing the essential observed weather and climate features of the Australia-New Zealand region with a good degree of accuracy, and further evaluation of extreme rainfall in the New Zealand region corroborated this (Rosier *et al* 2015). Additional evaluation tests shown in the supplementary materials (figures S1 and 2) further illustrate the adequacy of this modelling framework for the analysis presented in sections 3 and 4.

### 3. Results

#### 3.1. Best-estimate projections of annual rainfall change

Figure 1 shows ensemble mean changes in annual rainfall across the country, comparing projections of a modelled 3 °C world (hereafter ‘3 K experiment’) relative to simulations of the current climate (hereafter ‘Current Climate’ experiment). Consistent with evidence from past studies (MFE 2018, Bird *et al* 2023, Gibson *et al* 2024), annual mean rainfall is found to increase by up to 10% along the western coastline of both islands (particularly the South Island), while comparable decreases in annual rainfall can also be detected over drier inland regions of the South Island, particularly ‘rain shadow’ regions on the leeward side of the Southern Alps, like South Canterbury and Central Otago. Both patterns of change are consistent with a strengthening of rain-bearing weather systems arriving from the west of the country, while



no clear changes in annual rainfall can be seen across most of the North Island.

#### 3.2. Interrogating projected changes in rainfall on the driest and wettest days of the year

Next, we sort daily rainfall in each modelled year in descending order, examine this ordered wet-to-dry distribution of daily rainfall across each model year, and consider projected changes in daily rainfall for an individual location, focusing on the Northland region as a case study example (see red box in figure 1).

As illustrated in figure 2(a), we choose to focus on two periods of rainfall accumulation at the dry and wet end of the distribution, such that they each combine to result in the same amount of cumulative rainfall on an average year in the Current Climate experiment. Specifically, we focus on the most and fewest days needed to reach 25% of annual mean rainfall: for the case of Northland and considering the ensemble median of the Current Climate experiment, a quarter of annual rainfall can be reached by either combining the five wettest days of the year together (blue shading) or equally when considering total rainfall across the 326 driest days of the year (brown shading). Thus, we fix our subsequent analysis for this case study location to focus on the total rain which falls on the wettest five days (hereafter ‘wet quartile rainfall’) and on the driest 326 d

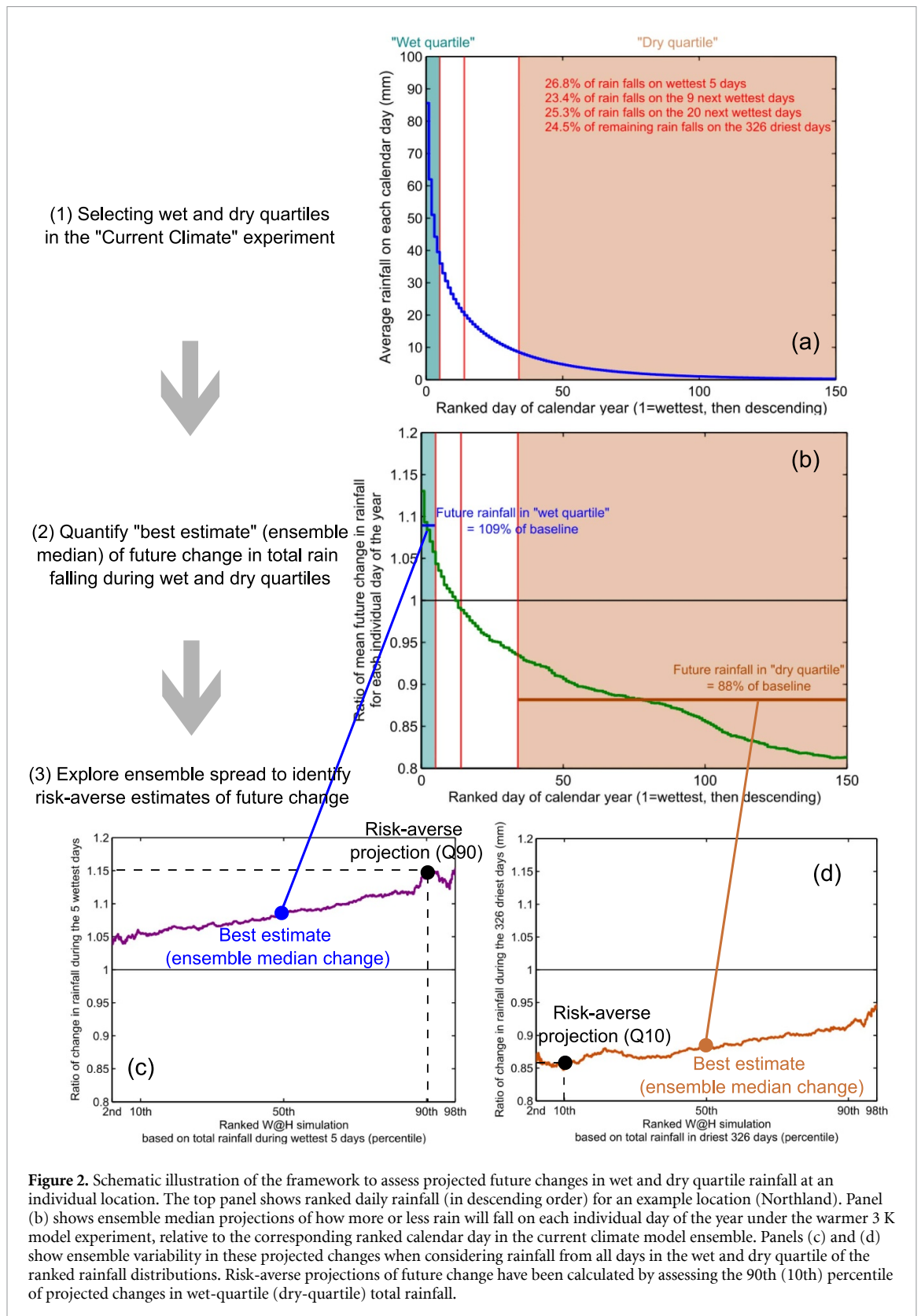


**Figure 2.** Schematic illustration of the framework to assess projected future changes in wet and dry quartile rainfall at an individual location. The top panel shows ranked daily rainfall (in descending order) for an example location (Northland). Panel (b) shows ensemble median projections of how more or less rain will fall on each individual day of the year under the warmer 3 K model experiment, relative to the corresponding ranked calendar day in the current climate model ensemble. Panels (c) and (d) show ensemble variability in these projected changes when considering rainfall from all days in the wet and dry quartile of the ranked rainfall distributions. Risk-averse projections of future change have been calculated by assessing the 90th (10th) percentile of projected changes in wet-quartile (dry-quartile) total rainfall.

of the year (hereafter 'dry quartile rainfall') for each individual ensemble member of both the Current Climate and 3 K experiments, as well as changes to rainfall for each ranked calendar day individually (note that days 151–360 have been excluded from

figure 2 as they are almost all days with zero rainfall). This framework enables the calculation and partitioning of how the proportion of annual rainfall coming from the wettest days will intensify in the warmer model experiment, relative to how total

rainfall coming from the driest days of the year will change.

Figure 2(b) shows the percent change in rainfall for each day of the year when comparing the median ensemble member of the 3 K experiment against the corresponding ensemble median output from the Current Climate experiment (see figure 2(a)). Again, this day-by-day comparison is made after first sorting daily rainfall in each model year in descending order. It is clear to see that the wettest days of the year are becoming wetter on average in the 3 K experiment, while the driest days of the year have less rainfall associated with them. When consolidating these changes for cumulative rainfall over both the five wettest and 326 driest days separately, we find wet quartile rainfall has increased by 9%, while total rainfall from the dry quartile reaches only 88% of that in the Current Climate experiment (a reduction of 12%).

Of course, the vast ensemble size of the multi-thousand member *Weather@Home* experiments allows the calculation of not just projected changes in daily rainfall for an ‘average’ year, but also changes in these daily rainfall distributions during unusually wet or dry years. Equally, we can view this exploration of the full model ensemble to produce a conservative (or ‘risk-averse’) assessment of projected changes for an average year in the 3 K experiments.

To demonstrate this, figures 2(c) and (d) show the spread of projected changes in wet and dry-quartile rainfall for all *Weather@Home* ensemble members, sorted along the  $x$ -axis on a quantile-quantile basis with respect to the total rain falling within each model year. For example, the Q90 point in figure 2(c) compares the percent intensification rate for the model year in the 3 K ensemble for which total rainfall across the five wettest days ranked in the 90th percentile of that ensemble, relative to the corresponding model year from the Current Climate experiment which also ranked in the 90th percentile in terms of total wet quartile rainfall. Equally, this can be thought of as comparing a 1-in-10-year wet year in the 3 K experiment against a 1-in-10-year wet year from the Current Climate experiment. After repeating this process for the dry end of the distribution—comparing model years drawn from the 10th percentile of each model ensemble based on total dry quartile rainfall—we then yield two alternative estimates of future changes in rainfall during the wettest and driest days of the year. Specifically, we find the wettest days on unusually wet years are becoming 15% more intense in the 3 K experiment relative to the Current Climate experiment (as opposed to 9% for the ensemble median), while dry quartile rainfall during unusually dry years in the 3 K experiment contributes only 85% of the total rainfall seen in the Current Climate experiment (as opposed to 88% for the ensemble median). We hereafter refer to these latter results as the risk-averse projections

of future change, while the ensemble-median projections presented in figure 2(b) are hereafter described as the best-estimate projections.

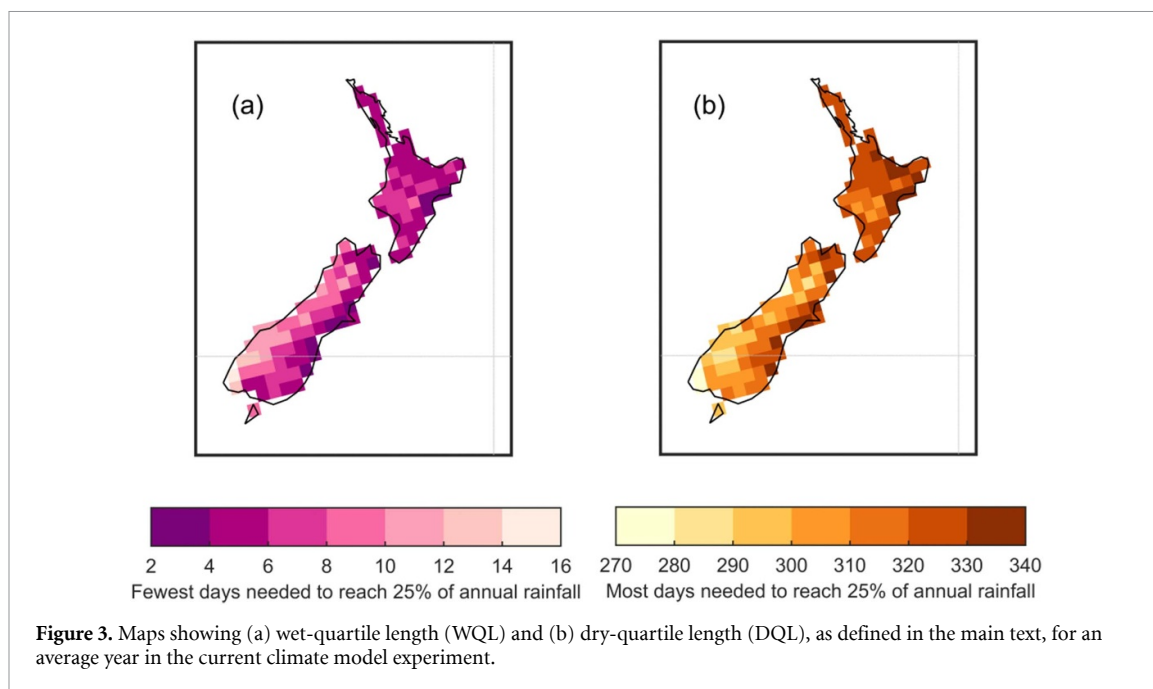
### 3.3. Decomposing nationwide projections of future rainfall on the wettest and driest days of the year

Extending the framework introduced in section 3.2 for each individual grid cell across New Zealand, we can extract changes in locally specific definitions of the wettest and driest days of the year, and their projected changes in corresponding total rainfall in response to additional global warming.

This first requires quantifying local variations in the least and the greatest number of calendar days required for cumulative rainfall to reach a quarter of annual mean rainfall in the Current Climate experiment. We hereafter refer to these values as wet quartile length (WQL) and dry quartile length (DQL), respectively: in the Northland case study example presented earlier in section 3.2, WQL was 5 d while DQL was 326 d. These local adjustments of what time periods are relevant to consider when contextualising changes to the wettest and driest days of the year allows a more meaningful comparison of future projections between regions with otherwise markedly different rainfall regimes.

#### 3.3.1. Spatial patterns of the least and greatest number of days needed to produce a quarter of annual mean rainfall

Figure 3 presents these spatial variations in WQL and DQL across New Zealand, revealing robust regional differences, particularly when comparing the climatologically dry eastern and wet western coastlines of the South Island. Indeed, many regions along the drier eastern coastlines of both islands reach a quarter of their annual rainfall from as little as two extremely wet days occurring. Most regions in the northern half of the North Island, including those regularly exposed to atmospheric rivers and extratropical cyclones impacting north-facing coastlines in the austral summertime (Rosier *et al* 2015, Stone *et al* 2024), see WQL values of between four and six days. Meanwhile, climatologically very wet regions in the south-west of country require the cumulative rain falling from their 16 wettest days before a quarter of annual rainfall is reached. Similar spatial patterns exist when considering DQL in figure 3(b), with DQL values varying from more than 330 d along the east coast of the North Island, between 320 and 330 d in the upper North Island, down to less than 280 d in the south-west of the country. As is clear from figure 3, the spatial patterns of WQL and DWL are themselves strongly negatively correlated ( $r = -0.94$ ), and consistent with corresponding regional patterns found in observations (see figures S1 and 2).



### 3.3.2. Spatially homogeneous patterns of projected rainfall change for local wettest and driest days of the year

Alongside projected changes in annual mean rainfall (as previously shown in figure 1), figure 4 presents maps of best-estimate and risk-averse projections of change in wet quartile and dry quartile total rainfall across New Zealand, with results from the 3 K experiment presented as a percentage of corresponding results from the Current Climate experiment.

When examining the best-estimate projections of wet-quartile and dry-quartile rainfall change, clear spatial patterns emerge. Of note, the additional rain falling during the wettest days of the year is uniformly increasing across nearly all locations in the 3 K ensemble, with most inland regions of the North Island showing 6%–10% additional rainfall, including many locations which have negligible projected change in total annual rainfall. Similarly homogeneous features are clear when assessing inland changes to total rainfall resulting from the driest days of the year: only about 80%–90% of total dry-quartile rainfall seen on average in the Current Climate experiment occurs in the 3 K world.

While these spatial characteristics of change are preserved, the magnitude of projected changes in wet-quartile and dry-quartile rainfall are otherwise exacerbated when comparing the risk-averse projections with the corresponding best-estimate projections. For example, those same inland regions of the North Island exhibit increases in wet-quartile rainfall of more than 10%, with values in excess of 15% along the western and northern coastlines of the North Island. Further, some regions of inland Marlborough

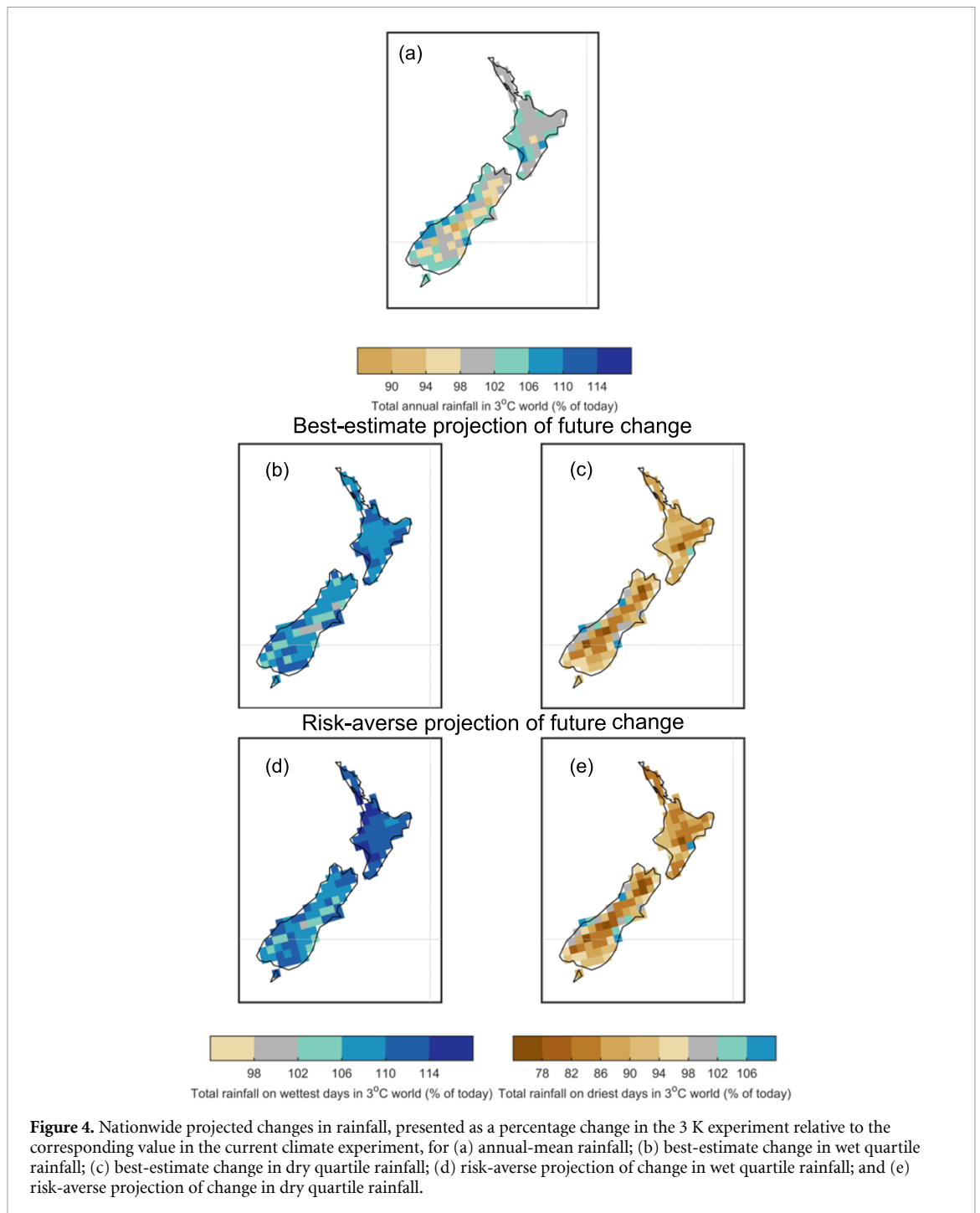
and Central Otago experience only 80% of the dry-quartile rainfall experienced in the Current Climate experiment under warmer conditions.

## 4. Discussion

### 4.1. Inferring future changes to the wettest and driest days of the year based on information about annual rainfall changes only

The ability to resolve robust changes in future rainfall for individual days of the year, as shown in sections 2 and 3, is enabled only by having exceptionally large model ensemble sizes, a beneficial feature of the distributed computing framework underpinning the *Weather@Home* regional climate modelling project. Indeed, computational cost is often the primary barrier to future climate projections credibly quantifying changes in weather extremes over centennial timescales: in essence, the number of ensemble members required to meaningfully resolve changes in the tails of rainfall and temperature distributions is too large to achieve while simultaneously providing projections of the evolution of twenty-first century climate under multiple different emissions scenarios. Thus, it is unrealistic to expect other regional climate modelling experiments which seek to project future changes in New Zealand climate at the local scale to be able to reproduce such specific insights about changes in daily rainfall characteristics.

To overcome the drawbacks of having smaller ensemble sizes, existing dynamically downscaled projections of future New Zealand climate coarsen the temporal scales on which they present information: for precipitation, this means a focus on season- or



annual-mean changes is commonplace. The results provided from this analysis offer a useful pathway to reconcile those annual-scale projections of rainfall change with meaningful information about what is happening on the wettest and driest days of the year. This is presented in figure 5 using scatter plots based on the location-specific results of figure 4, with each circle coloured according to the projected annual-mean rainfall change for that corresponding grid cell.

As figure 5 shows, we can produce an a priori estimate of how the statistics of daily rainfall are changing when only having information about how

annual-mean rainfall is changing at an individual location. In effect, a good first-order approximation when comparing an average year in a 3 degree world, relative to the current climate, is that locations which exhibit no change in annual-mean rainfall are likely to have their wettest days of the year producing 10% more rainfall when they occur, while the driest days of the year (dry-quartile total rainfall) will produce 10% less rain than in the current climate.

When applying a risk-averse lens to these a priori estimates of future change, these numbers increase further: for places where no annual-mean rainfall change is projected, on-the-ground decision-makers



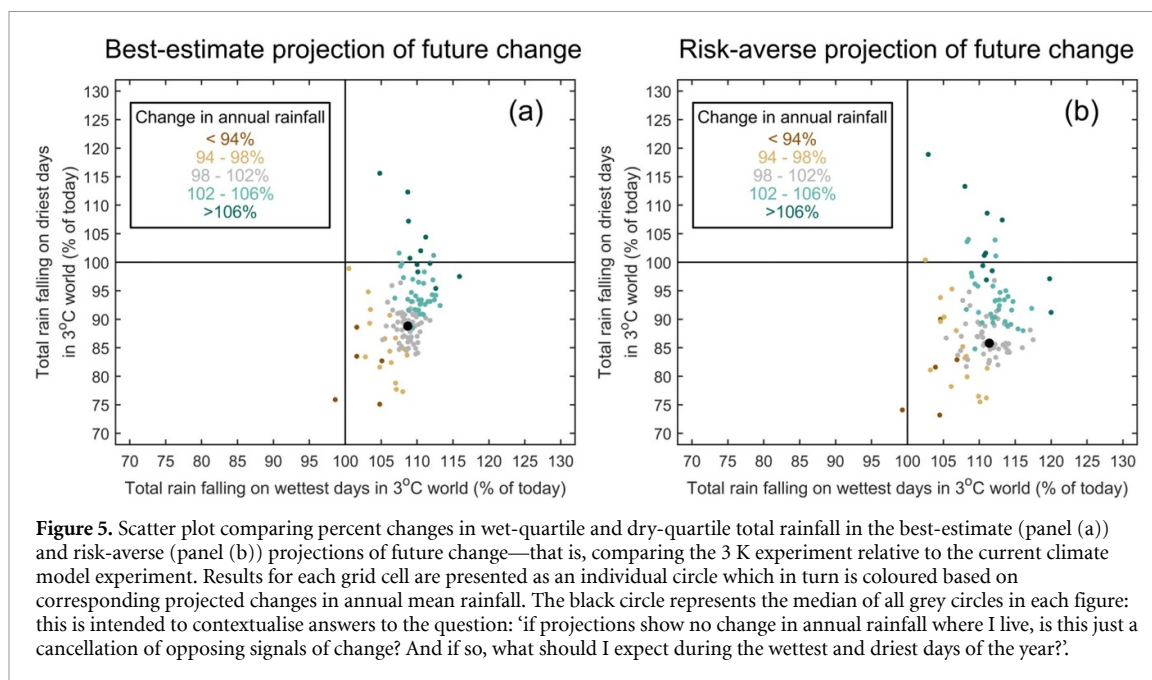


**Figure 5.** Scatter plot comparing percent changes in wet-quartile and dry-quartile total rainfall in the best-estimate (panel (a)) and risk-averse (panel (b)) projections of future change—that is, comparing the 3 K experiment relative to the current climate model experiment. Results for each grid cell are presented as an individual circle which in turn is coloured based on corresponding projected changes in annual mean rainfall. The black circle represents the median of all grey circles in each figure: this is intended to contextualise answers to the question: ‘if projections show no change in annual rainfall where I live, is this just a cancellation of opposing signals of change? And if so, what should I expect during the wettest and driest days of the year?’

should prepare for the driest days of the year (including modest-rainfall ‘drizzle days’, which are important in the context of drought) only contributing 85% of the total rainfall that they used to. Meanwhile, the wettest days of the year would produce approximately 12% more rainfall than the wettest days of the year in the current climate.

In lieu of more sophisticated large-ensemble model datasets, these ‘rules-of-thumb’ can serve as a powerful tool for on-the-ground decision makers to plan for what an average year might look like, in terms of wet and dry extremes, in a warmer 3 °C world, relative to the climate of the recent past. While beyond the scope of this analysis, it is worth noting that previous research found precipitation changes around the New Zealand region to scale approximately linearly with corresponding increases in global mean temperature (Seneviratne and Hauser 2020).

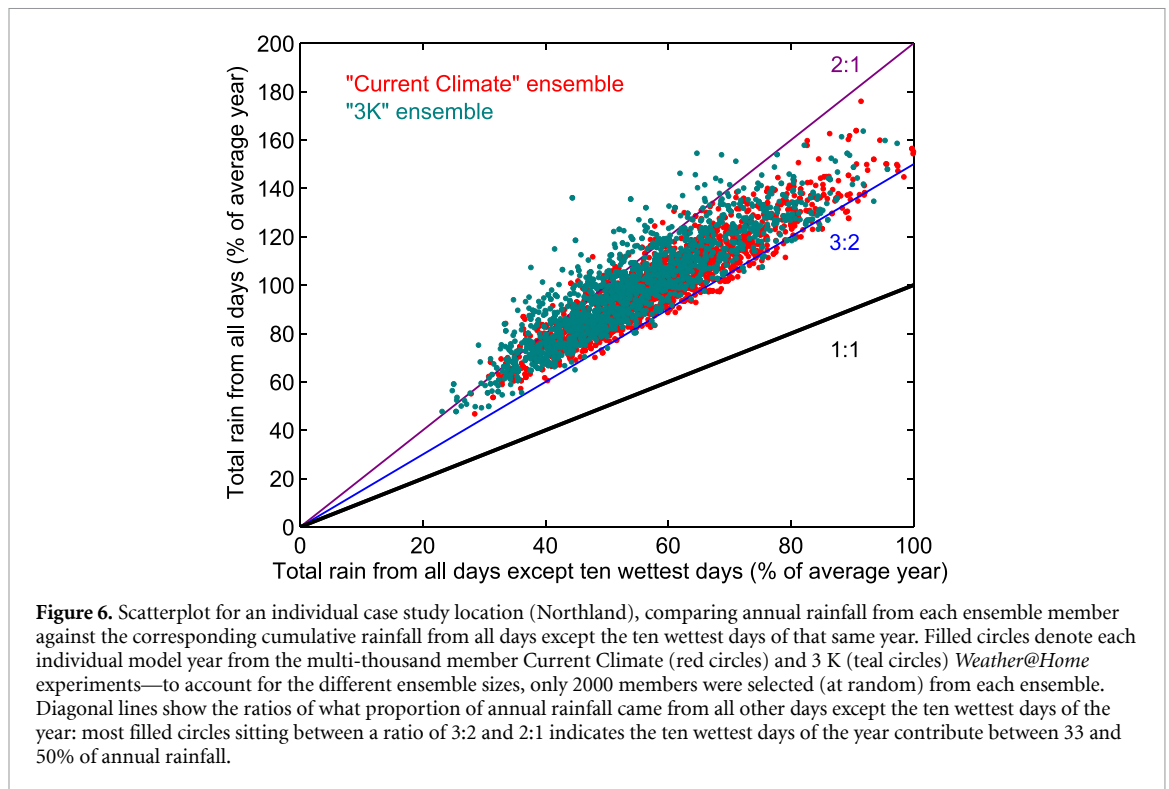
#### 4.2. Examining the implications for future dry year risk

Rank-ordering days of a calendar year based on total rainfall before examining projected future changes specific to each day has limitations in its utility, particularly when it comes to understanding the potential risks from real-world extreme events, like droughts. To further contextualise the interpretation of our results in a decision-relevant scenario, we examine the changing frequency of exceptionally dry years across our case study Northland region separately for all individual ensemble members (model years) from each experiment. To disentangle the relative impact of the wettest and driest days of the year changing differently in response to future warming, we compare total annual rainfall against

corresponding total rainfall from all days except the ten wettest days of the year in figure 6.

Figure 6 reveals these competing signals of change in the characteristics of daily rainfall manifest themselves in multiple different ways within the same location. First, there are multiple years in the 3 K experiment where total rainfall from the 350 driest days of the year contributes only some 40%–60% of annual mean rainfall, indicating a potentially high risk of recording exceptionally low cumulative rainfall for the year. And yet, these ensemble members (teal circles above the purple diagonal line in figure 6) end up being exceptionally wet years (20%–40% above normal): these model years are examples of where the wettest days of the year, supercharged because of the additional warming in the 3 K experiment, have produced more than half the year’s rainfall in only ten days and avoided any risks of a dry year occurring.

Conversely, there are other ensemble members within the 3 K experiment where little rain accumulates over the driest 350 d of the year, but this time accompanied by similarly modest rain falling on the ten wettest days of the year, resulting in a significantly dry year being recorded as a result. The probability of such an outcome is substantially elevated in the 3 K experiment, as evidenced by the large number of teal circles in the bottom-left corner of the scatter plot. Indeed, the number of model years with annual total rainfall reaching less than 60% of the ensemble mean climatology in this location increases three-fold in the warmer 3 K experiment, relative to the Current Climate ensemble. Comparable increases in the relative frequency of extreme dry years were also recorded in other regions with near-zero changes in annual rainfall (see figure S3).



This illustrative example demonstrates how even regions where the wettest days of the year are intensifying due to climate change can simultaneously experience elevated risks of extreme rainfall deficits. Future research is needed to explore other metrics of drought beyond annual rainfall, and how these are exacerbated in the warmer 3 K experiment, but such questions are beyond the scope of the current analysis.

#### 4.3. Limitations

It is important to acknowledge the limitations which are unavoidable when examining future climate projections based on output from only one type of regional climate model, even with the added benefit of multi-thousand member ensembles at a relatively high spatial resolution. As discussed elsewhere (Hawkins and Sutton 2009, Bellprat and Doblas-Reyes 2016, Deser *et al* 2020, Bevacqua *et al* 2023), model uncertainty inevitably contributes an additional layer of uncertainty in any future climate projections and this is particularly true when producing decision-relevant information at the regional scale (Giorgi 2019). The *Weather@Home* modelling framework partially overcomes this challenge by imposing multiple sea surface temperature boundary conditions from an array of different climate models, based on their independent projections of attributable change in sea surface temperatures with climate change (Black *et al* 2016, Mitchell *et al* 2017, Sparrow *et al* 2018). Similarly, the results presented in this analysis have been presented in a relative model framework wherever possible, so as to avoid any results being conditional on perfectly simulating observed

rainfall regimes around New Zealand. Nevertheless, the analyses in this study would benefit from repetition with other large ensembles of regional climate modelling, even though no such options currently exist which match *Weather@Home* for both ensemble size and model resolution over the New Zealand region.

## 5. Summary

By leveraging very large ensembles of regional model simulations for both the recent climate and in a world 3 °C warmer than pre-industrial levels, this analysis provides the first comprehensive assessment of changes to the characteristics of daily rainfall over New Zealand, for both the wettest and driest days of the year. Our results reveal that many locations around the country exhibit almost perfectly opposing signals of drying and wetting for the driest and wettest days of the year, resulting in many regions showing no projected change in annual rainfall.

For these regions with projections of no change in annual rainfall, the wettest days of the year—defined here as those days which combine to produce a quarter of annual rainfall in the current climate—will become at least 10% more intense in the 3 K model experiments, while corresponding dry-quartile rainfall decreases by an equivalent amount. Similarly, other regions which do show projected increases (decreases) in annual rainfall exhibit correspondingly larger signals of change in wet-quartile (dry-quartile) rainfall. When considering how these changes in daily rainfall express themselves in the form of dry-year

risk, we find robust increases in the number of years with ‘drought-busting’ extreme rainfall events, but also an approximate three-fold increase in the number of extreme dry years occurring. These projected increases in the volatility and unevenness of daily rainfall across New Zealand provide further evidence of the challenges which must be confronted if global temperatures continue to increase rapidly over the twenty-first century.

### Data availability statement

The data cannot be made publicly available upon publication because the cost of preparing, depositing and hosting the data would be prohibitive within the terms of this research project. The data that support the findings of this study are available upon reasonable request from the authors.

### Acknowledgments

The authors thank Daithi Stone for helpful discussions related to the manuscript. SMR and LJH acknowledge funding from the New Zealand Ministry for Business, Innovation & Employment’s (MBIE) via their Deep South National Science Challenge (Grant ID: C01X1412). LJH, DJF, TIM and SMR acknowledge further support from MBIE’s Endeavour Fund *Whakahura* programme (Grant ID: RTVU1906). LJH additionally acknowledges funding from Toka Tū Ake EQC (University Research Programme, Grant ID: URP3764) and MBIE’s Smart Ideas Fund (Grant ID: UOWX2302).

We would like to thank the Met Office Hadley Centre PRECIS team for their technical and scientific support for the development and application of *Weather@Home*. We would also like to thank Sarah Sparrow, David Wallom and the rest of the Oxford-based team who coordinate the *Weather@Home* project. Finally, we would like to thank all the volunteers who have donated their computing time to *climate-prediction.net* and *Weather@Home*.

### ORCID iDs

Luke J Harrington  <https://orcid.org/0000-0002-1699-6119>

Tom I Marsh  <https://orcid.org/0000-0003-3591-9810>

Dave J Frame  <https://orcid.org/0000-0002-0949-3994>

### References

- Allen M 1999 Do-it-yourself climate prediction *Nature* **401** 642  
 Anderson D P 2020 BOINC: a platform for volunteer computing *J. Grid Comput.* **18** 99–122

- Bellprat O and Doblas-Reyes F 2016 Attribution of extreme weather and climate events overestimated by unreliable climate simulations *Geophys. Res. Lett.* **43** 2158–64  
 Bevacqua E, Suarez-Gutierrez L, Jézéquel A, Lehner F, Vrac M, Yiou P and Zscheischler J 2023 Advancing research on compound weather and climate events via large ensemble model simulations *Nat. Commun.* **14** 2145  
 Bird L J, Bodeker G E and Clem K R 2023 Sensitivity of extreme precipitation to climate change inferred using artificial intelligence shows high spatial variability *Commun. Earth Environ.* **4** 1–14  
 Black M T *et al* 2016 The weather@home regional climate modelling project for Australia and New Zealand *Geosci. Model Dev.* **9** 3161–76  
 Craddock-Henry N A, Frame B, Preston B L, Reisinger A and Rothman D S 2018 Dynamic adaptive pathways in downscaled climate change scenarios *Clim. Change* **150** 333–41  
 Deser C *et al* 2020 Insights from Earth system model initial-condition large ensembles and future prospects *Nat. Clim. Change* **10** 277–86  
 Donlon C J, Martin M, Stark J, Roberts-Jones J, Fiedler E and Wimmer W 2012 The operational sea surface temperature and sea ice analysis (OSTIA) system *Remote Sens. Environ.* **116** 140–58  
 Evans J P, Di Virgilio G, Hirsch A L, Hoffmann P, Remedio A R, Ji F, Rockel B and Coppola E 2021 The CORDEX-Australasia ensemble: evaluation and future projections *Clim. Dyn.* **57** 1385–401  
 Eyring V, Bony S, Meehl G A, Senior C A, Stevens B, Stouffer R J and Taylor K E 2016 Overview of the coupled model intercomparison project phase 6 (CMIP6) experimental design and organization *Geosci. Model Dev.* **9** 1937–58  
 Fishman R 2016 More uneven distributions overturn benefits of higher precipitation for crop yields *Environ. Res. Lett.* **11** 024004  
 Gibson P B, Rampal N, Dean S M and Morgenstern O 2024 Storylines for future projections of precipitation over New Zealand in CMIP6 models *J. Geophys. Res.* **129** e2023JD039664  
 Giorgi F 2019 Thirty years of regional climate modeling: where are we and where are we going next? *J. Geophys. Res. Atmos.* **124** 5696–723  
 Giorgi F, Im E-S, Coppola E, Diffenbaugh N S, Gao X J, Mariotti L and Shi Y 2011 Higher hydroclimatic intensity with global warming *J. Clim.* **24** 5309–24  
 Goffin B D, Kansara P and Lakshmi V 2024 Intensification in the wettest days to 50% of annual precipitation (WD50) across Europe *Geophys. Res. Lett.* **51** e2023GL107403  
 Gudmundsson L *et al* 2021 Globally observed trends in mean and extreme river flow attributed to climate change *Science* **371** 1159–62  
 Harrington L J 2021 Temperature emergence at decision-relevant scales *Environ. Res. Lett.* **16** 094018  
 Hawkins E and Sutton R 2009 The potential to narrow uncertainty in regional climate predictions *Bull. Am. Meteorol. Soc.* **90** 1095–107  
 Jones R, Noguer M, Hassell D, Hudson D, Wilson S, Jenkins G and Mitchell J 2004 *Generating High-Resolution Climate Change Scenarios Using PRECIS* (Met Office Hadley Centre)  
 Lehner F, Deser C, Maher N, Marotzke J, Fischer E M, Brunner L, Knutti R and Hawkins E 2020 Partitioning climate projection uncertainty with multiple large ensembles and CMIP5/6 *Earth Syst. Dyn.* **11** 491–508  
 Lesk C, Anderson W, Rigden A, Coast O, Jägermeyr J, McDermid S, Davis K F and Konar M 2022 Compound heat and moisture extreme impacts on global crop yields under climate change *Nat. Rev. Earth Environ.* **3** 872–89  
 Lo Y T E *et al* 2019 Increasing mitigation ambition to meet the Paris Agreement’s temperature goal avoids substantial heat-related mortality in U.S. cities *Sci. Adv.* **5** eaau4373

- Massey N, Jones R, Otto F E L, Aina T, Wilson S, Murphy J M, Hassell D, Yamazaki Y H and Allen M R 2015 weather@home—development and validation of a very large ensemble modelling system for probabilistic event attribution *Q.J.R. Meteorol. Soc.* **141** 1528–45
- Ministry for the Environment 2018 *Climate Change Projections for New Zealand: Atmospheric Projections Based on Simulations from the IPCC Fifth Assessment Report* (Ministry for the Environment) (available at: [www.mfe.govt.nz/sites/default/files/media/Climate%20Change/Climate-change-projections-2nd-edition-final.pdf](http://www.mfe.govt.nz/sites/default/files/media/Climate%20Change/Climate-change-projections-2nd-edition-final.pdf))
- Mitchell D *et al* 2017 Half a degree additional warming, prognosis and projected impacts (HAPPI): background and experimental design *Geosci. Model Dev.* **10** 571–83
- Padrón R S, Gudmundsson L, Decharme B, Ducharne A, Lawrence D M, Mao J, Peano D, Krinner G, Kim H and Seneviratne S I 2020 Observed changes in dry-season water availability attributed to human-induced climate change *Nat. Geosci.* **13** 477–81
- Pendergrass A G 2018 What precipitation is extreme? *Science* **360** 1072–3
- Pendergrass A G and Knutti R 2018 The uneven nature of daily precipitation and its change *Geophys. Res. Lett.* **45** 11,980–8
- Pendergrass A G, Knutti R, Lehner F, Deser C and Sanderson B M 2017 Precipitation variability increases in a warmer climate *Sci. Rep.* **7** 17966
- Pope V D, Gallani M L, Rowntree P R and Stratton R A 2000 The impact of new physical parametrizations in the Hadley Centre climate model: hadAM3 *Clim. Dyn.* **16** 123–46
- Rosier S, Dean S, Stuart S, Carey-Smith T, Black M T and Massey N 2015 Extreme rainfall in early July 2014 in Northland, New Zealand—was there an Anthropogenic Influence? *Bull. Am. Meteorol. Soc.* **96** S136–40
- Seneviratne S I and Hauser M 2020 Regional climate sensitivity of climate extremes in CMIP6 versus CMIP5 multimodel ensembles *Earth's Future* **8** e2019EF001474
- Shiogama H, Hirata R, Hasegawa T, Fujimori S, Ishizaki N N, Chatani S, Watanabe M, Mitchell D and Lo Y T E 2020 Historical and future anthropogenic warming effects on droughts, fires and fire emissions of CO<sub>2</sub> and PM<sub>2.5</sub> in equatorial Asia when 2015-like El Niño events occur *Earth Syst. Dyn.* **11** 435–45
- Sloat L L, Gerber J S, Samberg L H, Smith W K, Herrero M, Ferreira L G, Godde C M and West P C 2018 Increasing importance of precipitation variability on global livestock grazing lands *Nat. Clim. Change* **8** 214–8
- Sparrow S *et al* 2018 Attributing human influence on the July 2017 Chinese heatwave: the influence of sea-surface temperatures *Environ. Res. Lett.* **13** 114004
- Stone D, Noble C, Bodeker G E, Dean S, Harrington L J, Rosier S M, Rye G and Tradowsky J S 2024 Cyclone Gabrielle as a design storm for northeastern Aotearoa New Zealand under anthropogenic warming *Earth's Future (Accepted)*
- Sturman A P and Tapper N J 2006 *The Weather and Climate of Australia and New Zealand* (Oxford University Press) (available at: <https://research.monash.edu/en/publications/the-weather-and-climate-of-australia-and-new-zealand>)
- Taylor K E, Stouffer R J and Meehl G A 2012 An overview of CMIP5 and the experiment design *Bull. Am. Meteorol. Soc.* **93** 485–98